An Implicit Keller Box Numerical Scheme for the Solution of Fractional Subdiffusion Equations☆

S. A. Osman[a], T. A. M. Langlands[a,*]

[a] *University of Southern Queensland, Toowoomba, QLD 4350, Australia*

Abstract

In this work, we present a new implicit numerical scheme for fractional subdiffusion equations. In this approach we use the Keller Box method [1] to spatially discretise the fractional subdiffusion equation and we use a modified L1 scheme (ML1), similar to the L1 scheme originally developed by Oldham and Spanier [2], to approximate the fractional derivative. The stability of the proposed method was investigated by using Von-Neumann stability analysis. We have proved the method is unconditionally stable when $0 < \lambda_q < \min(\frac{1}{\mu_0}, 2^\gamma)$ and $0 < \gamma \leq 1$, and demonstrated the method is also stable numerically in the case $\frac{1}{\mu_0} < \lambda_q \leq 2^\gamma$ and $\log_3 2 \leq \gamma \leq 1$. The accuracy and convergence of the scheme was also investigated and found to be of order $O(\Delta t^{1+\gamma})$ in time and $O(\Delta x^2)$ in space. To confirm the accuracy and stability of the proposed method we provide three examples with one including a linear reaction term.

Keywords: Fractional subdiffusion equation, Keller Box method, Fractional calculus, L1 scheme, Linear reaction.

1. Introduction

Anomalous subdiffusion is a physical phenomenon which observed in many systems which involve trapping, binding or macromolecular crowding. In recent years, examples of anomalous diffusion have been discovered in many different fields such as fluid mechanics [3, 4], physics [5, 6, 7, 8], engineering and biology [9, 10, 11, 12]. Anomalous subdiffusion can be modelled using Continuous Time Random Walks (CTRWs), and using fractional partial differential equations

*Corresponding author
Email addresses: sheelan.osman@usq.edu.au (S. A. Osman), Trevor.Langlands@usq.edu.au (T. A. M. Langlands)

(FPDEs) [7, 13]. One of the well-known FPDEs is the fractional subdiffusion equation [7]

$$\frac{\partial u}{\partial t} = K_\gamma \frac{\partial^{1-\gamma}}{\partial t^{1-\gamma}} \left(\frac{\partial^2 u}{\partial x^2} \right). \tag{1}$$

In Eq. (1), K_γ is the anomalous diffusion coefficient and γ is the anomalous diffusion exponent, which in the case of the subdiffusion equation, lies in the interval $0 < \gamma < 1$. What sets Eq. (1) apart from the standard diffusion equation is the presence of the fractional derivative operator, $\frac{\partial^{1-\gamma}}{\partial t^{1-\gamma}}$, which operates on the Laplacian term. In this article we use the Riemann–Liouville fractional derivative [14] which is defined as

$$\frac{\partial^{1-\gamma} g(t)}{\partial t^{1-\gamma}} = \frac{1}{\Gamma(\gamma)} \frac{d}{dt} \int_0^t \frac{g(\tau)}{(t-\tau)^{1-\gamma}} d\tau, \tag{2}$$

where $\Gamma(.)$ is the Gamma function and $0 < \gamma \leq 1$.

Numerical techniques are required to find the approximate solution of FPDEs because the closed form analytic solutions either do not exist or involve special functions, such as the Fox (H-function) function [15] and the Mittag–Leffler function [14], which are difficult to evaluate. As a consequence many researchers have developed numerical schemes to approximate the solution of FPDEs such as the fractional subdiffusion equation in Eq. (1). The majority of these schemes can be split into either explicit type methods [16, 17, 18, 19, 20, 21] or implicit numerical methods [22, 18, 23, 24, 25, 21, 26].

Langlands and Henry [22] considered an implicit method for the fractional subdiffusion equation using the L1 approximation to estimate the fractional derivative. They discussed the accuracy and stability for the numerical method and showed the method is stable and convergent of order $O(\Delta t^{1+\gamma}) + O(\Delta x^2)$. Stability of this method was later proven by Chen et al. [27] using an energy 2-norm approach.

More accurate numerical methods are available for the subdiffusion equation if it is rewritten in the form

$$\frac{\partial^\gamma u}{\partial t^\gamma} = K_\gamma \frac{\partial^2 u}{\partial x^2}, \tag{3}$$

using a Caputo fractional derivative on the left hand side [28, 29, 30, 31]. The advantage of this form is that there is only one temporal derivative to approximate instead of two as in the Eq. (1) form. However, our method could be used for more general equations such as the fractional cable equation [8]

$$\frac{\partial u}{\partial t} = \frac{\partial^{1-\gamma}}{\partial t^{1-\gamma}} \left(\frac{\partial^2 u}{\partial x^2} \right) - \alpha u, \tag{4}$$

where we cannot rewrite the equation with the fractional derivative on the left hand side.

The Keller Box method is an implicit numerical scheme which is second order accurate in both space and time for the standard diffusion equation [32]. The idea of the Keller Box method is to replace the higher spatial derivatives in the equation by the first derivative of an introduced additional variable. Al-Shibani [33] proposed a Keller Box method for the one dimensional time fractional diffusion equation in Eq. (3) where the Grünwald–Letnikov approximation was applied to approximate the fractional derivative.

In this article we develop an alternative numerical method based upon the Keller Box Method [1] for the subdiffusion equation in Eq. (1) modified to include a source term $f(x,t)$

$$\frac{\partial u}{\partial t} = K_\gamma \frac{\partial^{1-\gamma}}{\partial t^{1-\gamma}} \left(\frac{\partial^2 u}{\partial x^2} \right) + f(x,t) \tag{5}$$

which we will solve on the finite spatial domain $0 \leq x \leq L$ and for times $0 \leq t \leq T$ subject to the following the initial and boundary conditions

$$u(x,0) = g(x), \qquad 0 < x < L, \tag{6}$$

$$u(0,t) = \varphi_1(t) \quad \text{and} \quad u(L,t) = \varphi_2(t), \qquad 0 < t \leq T \ . \tag{7}$$

Let $\Omega = \{(x,t) | 0 \leq x \leq L, 0 \leq t \leq T\}$ and then we define the function space

$$G(\Omega) = \left\{ \theta(x,t) \middle| \frac{\partial^2 \theta(x,t)}{\partial x^2} \in C^2(\Omega), \text{ and } \frac{\partial^5 \theta(x,t)}{\partial x^4 \partial t} \in C(\Omega) \right\}. \tag{8}$$

We suppose that the continuous problem Eqs. (5) – (7) has a smooth solution $u(x_i, t_j) \in G(\Omega)$. This scheme extends the standard approach to the fractional case where the Riemann-Liouville definition of the fractional derivative is used on the right side of the equation instead of Caputo definition used by Al-Shibani [33]. In addition, we use a modification of the L1 scheme [2] to approximate the fractional derivative instead of the Grünwald-Letnikov approximation used by Al-Shibani [33]. In the next section we develop the modified scheme and in later sections we investigate the stability and the accuracy of the implicit numerical method and give examples of its implementation.

2. Derivation of the numerical method

In this section we develop an implicit numerical scheme using the Keller Box method to spatially discretise Eq. (5) and a modification of the L1 scheme to approximate the Riemann–Liouville

fractional derivative. For positive integers M and N, we define the spatial grid points, x_i as $\{x_i | \, 0 = x_1 < x_2 < x_3 < \cdots < x_{N-1} < x_N = L\}$, where we denote $\Delta x_i = x_i - x_{i-1}$ as the spatial grid spacing. We also use equally spaced temporal points as $t_j = j\Delta t$, $j = 0, 1, \ldots, M$ with $\Delta t = T/M$ which denotes the time step size.

Following the Keller Box approach, we approximate Eq. (5) at the point $x_{i-\frac{1}{2}}$ and time $t_{j+\frac{1}{2}}$ as

$$\left[\frac{\partial u}{\partial t}\right|_{i-\frac{1}{2}}^{j+\frac{1}{2}} = K_\gamma \left[\frac{\partial^{1-\gamma}}{\partial t^{1-\gamma}}\left(\frac{\partial^2 u}{\partial x^2}\right)\right|_{i-\frac{1}{2}}^{j+\frac{1}{2}} + f\left(x_{i-\frac{1}{2}}, t_{j+\frac{1}{2}}\right) \, , \tag{9}$$

where u_i^j is the numerical approximation of the exact solution $U_i^j = u(x_i, t_j)$ at the discrete grid point (x_i, t_j). We approximate the value of the fractional derivative at the time $t_{j+\frac{1}{2}}$ in Eq. (9) by using the ML1 scheme, developed in [34], which is given by

$$\begin{aligned}\left[\frac{d^{1-\gamma} g(t)}{dt^{1-\gamma}}\right|_{ML1}^{j+\frac{1}{2}} = \frac{\Delta t^{\gamma-1}}{\Gamma(1+\gamma)} \Bigg\{ & \beta_j(\gamma) g(0) + 2\left(\frac{1}{2}\right)^\gamma \left(g(t_{j+\frac{1}{2}}) - g(t_j)\right) \\ & + \sum_{k=1}^{j} \mu_{j-k}(\gamma) \left(g(t_k) - g(t_{k-1})\right) \Bigg\} \, ,\end{aligned} \tag{10}$$

with the weights

$$\beta_j(\gamma) = \gamma\left(j + \frac{1}{2}\right)^{\gamma-1} \quad \text{and} \qquad \mu_j(\gamma) = \left(j + \frac{3}{2}\right)^\gamma - \left(j + \frac{1}{2}\right)^\gamma . \tag{11}$$

The ML1 scheme is shown by Osman [34] to be convergent of order $O(\Delta t^{1+\gamma})$ for function $g(t) \in C^2[0, t_{j+\frac{1}{2}}]$, which is a similar convergence order for the scheme given in [35]. The scheme in [35] is similar to the ML1 scheme but uses different weights and involves the evaluation at the midpoints $t_{k+\frac{1}{2}}$, where $k = 0, 1, 2, \ldots, j$.

2.1. Keller Box method with the ML1 scheme

In this section, the numerical scheme for solving Eq. (5) will be developed using the idea of the Keller Box method combined with the approximation of the fractional derivative in Eqs. (10) – (11). First we define the first spatial derivative in Eq. (5) by

$$\left[\frac{\partial u}{\partial x}\right|_{i-\frac{1}{2}}^{j+1} = v_{i-\frac{1}{2}}^{j+1}. \tag{12}$$

Using Eqs. (10) and (12), Eq. (5) can be rewritten as

$$\left[\frac{\partial u}{\partial t}\right|_{i-\frac{1}{2}}^{j+\frac{1}{2}} = \frac{K_\gamma \Delta t^{\gamma-1}}{\Gamma(1+\gamma)} \left\{ \beta_j(\gamma) \left[\frac{\partial v}{\partial x}\right|_{i-\frac{1}{2}}^{0} + 2\left(\frac{1}{2}\right)^\gamma \left(\left[\frac{\partial v}{\partial x}\right|_{i-\frac{1}{2}}^{j+\frac{1}{2}} - \left[\frac{\partial v}{\partial x}\right|_{i-\frac{1}{2}}^{j} \right) + \sum_{k=1}^{j} \mu_{j-k}(\gamma) \left(\left[\frac{\partial v}{\partial x}\right|_{i-\frac{1}{2}}^{k} - \left[\frac{\partial v}{\partial x}\right|_{i-\frac{1}{2}}^{k-1} \right) \right\} + f\left(x_{i-\frac{1}{2}}, t_{j+\frac{1}{2}}\right) \ . \tag{13}$$

Following the Keller Box method [32, 36] we next approximate the first order spatial and temporal derivatives in Eqs. (12) and (13) using centred finite difference approximations, to find

$$\frac{u_i^{j+1} - u_{i-1}^{j+1}}{\Delta x_i} = v_{i-\frac{1}{2}}^{j+1} \ , \tag{14}$$

and

$$\frac{u_{i-\frac{1}{2}}^{j+1} - u_{i-\frac{1}{2}}^{j}}{\Delta t} = \frac{K_\gamma \Delta t^{\gamma-1}}{\Gamma(1+\gamma)} \left\{ \beta_j(\gamma) \left(\frac{v_i^0 - v_{i-1}^0}{\Delta x_i} \right) + 2\left(\frac{1}{2}\right)^\gamma \left(\frac{v_i^{j+\frac{1}{2}} - v_{i-1}^{j+\frac{1}{2}}}{\Delta x_i} \right) -2\left(\frac{1}{2}\right)^\gamma \left(\frac{v_i^{j} - v_{i-1}^{j}}{\Delta x_i} \right) + \sum_{k=1}^{j} \mu_{j-k}(\gamma) \left(\frac{v_i^{k} - v_{i-1}^{k}}{\Delta x_i} - \frac{v_i^{k-1} - v_{i-1}^{k-1}}{\Delta x_i} \right) \right\} + [f]_{i-\frac{1}{2}}^{j+\frac{1}{2}} \ . \tag{15}$$

Now replacing the $v_i^{j+\frac{1}{2}}$, and $v_{i-\frac{1}{2}}^{j}$ terms by their corresponding temporal and spatial averages, gives the equations

$$\frac{u_i^{j+1} - u_{i-1}^{j+1}}{\Delta x_i} = \frac{v_i^{j+1} + v_{i-1}^{j+1}}{2} \ , \tag{16}$$

and

$$\frac{u_i^{j+1} + u_{i-1}^{j+1}}{2\Delta t} = \frac{u_i^{j} + u_{i-1}^{j}}{2\Delta t} + \frac{K_\gamma \Delta t^{\gamma-1}}{\Gamma(1+\gamma)} \left\{ \frac{\beta_j(\gamma)}{\Delta x_i} \left(v_i^0 - v_{i-1}^0 \right) + \frac{\left(\frac{1}{2}\right)^\gamma}{\Delta x_i} \left(v_i^{j+1} - v_{i-1}^{j+1} \right) -\frac{\left(\frac{1}{2}\right)^\gamma}{\Delta x_i} \left(v_i^{j} - v_{i-1}^{j} \right) + \frac{1}{\Delta x_i} \sum_{k=1}^{j} \mu_{j-k}(\gamma) \left[v_i^{k} - v_{i-1}^{k} - \left(v_i^{k-1} - v_{i-1}^{k-1} \right) \right] \right\} + [f]_{i-\frac{1}{2}}^{j+\frac{1}{2}} \, . \tag{17}$$

Solving Eq. (16) to find v_{i-1}^j and combining with Eq. (17) gives the equation for u_i^j and v_i^j

$$\begin{aligned} \frac{u_i^{j+1} + u_{i-1}^{j+1}}{2\Delta t} = \frac{u_i^{j} + u_{i-1}^{j}}{2\Delta t} + \frac{2K_\gamma \Delta t^{\gamma-1}}{\Gamma(1+\gamma)} \Bigg\{ & \frac{\beta_j(\gamma)}{\Delta x_i} v_i^0 - \frac{\beta_j(\gamma)}{(\Delta x_i)^2} \left(u_i^0 - u_{i-1}^0 \right) - \frac{\left(\frac{1}{2}\right)^\gamma}{(\Delta x_i)^2} \left(u_i^{j+1} - u_{i-1}^{j+1} \right) \\ & + \frac{\left(\frac{1}{2}\right)^\gamma}{\Delta x_i} v_i^{j+1} + \frac{\left(\frac{1}{2}\right)^\gamma}{(\Delta x_i)^2} \left(u_i^{j} - u_{i-1}^{j} \right) - \frac{\left(\frac{1}{2}\right)^\gamma}{\Delta x_i} v_i^{j} + \frac{1}{\Delta x_i} \sum_{k=1}^{j} \mu_{j-k}(\gamma) \left(v_i^{k} - v_i^{k-1} \right) \\ & - \frac{1}{(\Delta x_i)^2} \sum_{k=1}^{j} \mu_{j-k}(\gamma) \left[u_i^{k} - u_{i-1}^{k} - \left(u_i^{k-1} - u_{i-1}^{k-1} \right) \right] \Bigg\} + [f]_{i-\frac{1}{2}}^{j+\frac{1}{2}} \, . \end{aligned} \tag{18}$$

In a similar manner, by replacing i by $i+1$ in Eqs. (16) and (17), and the eliminating v_{i+1}^j we then have a second equation

$$\begin{aligned}\frac{u_{i+1}^{j+1}+u_i^{j+1}}{2\Delta t} &= \frac{u_{i+1}^j+u_i^j}{2\Delta t}+\frac{2K_\gamma\Delta t^{\gamma-1}}{\Gamma(1+\gamma)}\left\{\frac{\beta_j(\gamma)}{(\Delta x_{i+1})^2}\left(u_{i+1}^0-u_i^0\right)-\frac{\beta_j(\gamma)}{\Delta x_{i+1}}v_i^0+\frac{\left(\frac{1}{2}\right)^\gamma}{(\Delta x_{i+1})^2}\left(u_{i+1}^{j+1}-u_i^{j+1}\right)\right.\\ &-\frac{\left(\frac{1}{2}\right)^\gamma}{\Delta x_{i+1}}v_i^{j+1}-\frac{\left(\frac{1}{2}\right)^\gamma}{(\Delta x_{i+1})^2}\left(u_{i+1}^j-u_i^j\right)+\frac{\left(\frac{1}{2}\right)^\gamma}{\Delta x_{i+1}}v_i^j-\frac{1}{\Delta x_{i+1}}\sum_{k=1}^{j}\mu_{j-k}(\gamma)\left(v_i^k-v_i^{k-1}\right)\\ &\left.+\frac{1}{(\Delta x_{i+1})^2}\sum_{k=1}^{j}\mu_{j-k}(\gamma)\left[u_{i+1}^k-u_i^k-\left(u_{i+1}^{k-1}-u_i^{k-1}\right)\right]\right\}+[f]_{i+\frac{1}{2}}^{j+\frac{1}{2}}. \end{aligned}\tag{19}$$

Combining Eqs. (18) and (19) gives an equation for u_i^{j+1} alone

$$\begin{aligned}&\frac{1}{2\Delta t}\left(\Delta x_{i+1}u_{i+1}^{j+1}+\left(\Delta x_{i+1}+\Delta x_i\right)u_i^{j+1}+\Delta x_i u_{i-1}^{j+1}\right)\\ &\quad-\frac{2K_\gamma\Delta t^{\gamma-1}}{\Delta x_{i+1}\Delta x_i\Gamma(1+\gamma)}\left(\frac{1}{2}\right)^\gamma\left(\Delta x_i u_{i+1}^{j+1}+\left(\Delta x_i+\Delta x_{i+1}\right)u_i^{j+1}+\Delta x_{i+1}u_{i-1}^{j+1}\right)\\ &=\frac{1}{2\Delta t}\left(\Delta x_{i+1}u_{i+1}^{j}+\left(\Delta x_{i+1}+\Delta x_i\right)u_i^{j}+\Delta x_i u_{i-1}^{j}\right)\\ &-\frac{2K_\gamma\Delta t^{\gamma-1}}{\Delta x_{i+1}\Delta x_i\Gamma(1+\gamma)}\left(\frac{1}{2}\right)^\gamma\left[\Delta x_i u_{i+1}^{j}+\left(\Delta x_i+\Delta x_{i+1}\right)u_i^{j}+\Delta x_{i+1}u_{i-1}^{j}\right]\\ &+\frac{2K_\gamma\Delta t^{\gamma-1}}{\Delta x_{i+1}\Delta x_i\Gamma(1+\gamma)}\left\{\beta_j(\gamma)\left[\Delta x_i\left(u_{i+1}^0-u_i^0\right)-\Delta x_{i+1}\left(u_i^0-u_{i-1}^0\right)\right]\right.\\ &-\Delta x_{i+1}\sum_{k=1}^{j}\mu_{j-k}(\gamma)\left[\left(u_i^k-u_{i-1}^k\right)-\left(u_i^{k-1}-u_{i-1}^{k-1}\right)\right]+\Delta x_i\sum_{k=1}^{j}\mu_{j-k}(\gamma)\left[\left(u_{i+1}^k-u_i^k\right)\right.\\ &\left.\left.-\left(u_{i+1}^{k-1}-u_i^{k-1}\right)\right]\right\}+\Delta x_i\,[f]_{i-\frac{1}{2}}^{j+\frac{1}{2}}+\Delta x_{i+1}\,[f]_{i+\frac{1}{2}}^{j+\frac{1}{2}}. \end{aligned}\tag{20}$$

In the case of constant grid spacing $\Delta x_i=\Delta x$, Eq. (20) simplifies to

$$\begin{aligned}&\left(u_{i+1}^{j+1}+2u_i^{j+1}+u_{i-1}^{j+1}\right)-\left(\frac{1}{2}\right)^\gamma d\left(u_{i+1}^{j+1}-2u_i^{j+1}+u_{i-1}^{j+1}\right)\\ &=\left(u_{i+1}^{j}+2u_i^{j}+u_{i-1}^{j}\right)-\left(\frac{1}{2}\right)^\gamma d\left(u_{i+1}^{j}-2u_i^{j}+u_{i-1}^{j}\right)+d\beta_j(\gamma)\left(u_{i+1}^0-2u_i^0+u_{i-1}^0\right)\\ &+d\sum_{k=1}^{j}\mu_{j-k}(\gamma)\left[u_{i+1}^k-2u_i^k+u_{i-1}^k-\left(u_{i+1}^{k-1}-2u_i^{k-1}+u_{i-1}^{k-1}\right)\right]+2\Delta t\left([f]_{i-\frac{1}{2}}^{j+\frac{1}{2}}+[f]_{i+\frac{1}{2}}^{j+\frac{1}{2}}\right), \end{aligned}\tag{21}$$

where

$$d=\frac{4K_\gamma\Delta t^\gamma}{\Delta x^2\Gamma(1+\gamma)}.\tag{22}$$

We refer to this scheme as the KBML1 method. If we set $\gamma=1$, noting $\beta_j(1)=1$ and $\mu_{j-k}(1)=1$, Eq. (21) reduces to the Keller Box method [32] for diffusion equation in the case of a nonzero source term.

3. The accuracy of the numerical method

In this section we consider the accuracy of the KBML1 scheme given by Eq. (21). Suppose that $U_i^j = u(x_i, t_j) \in G(\Omega)$, where $i = 1, \ldots, N$ and $j = 1, \ldots, M$, be the exact solution of the problem Eqs. (5) – (7) at the point (x_i, t_j). To begin we rewrite Eq. (21) as

$$\frac{1}{\Delta t}\left[U_i^{j+1} - U_i^j\right] = K_\gamma \left[\frac{\partial^{1-\gamma}}{\partial t^{1-\gamma}}\left(\frac{\partial^2 U}{\partial x^2}\right)\Big|_i^{j+\frac{1}{2}} + \left(\frac{1}{2}\right)^\gamma \frac{K_\gamma \Delta t^{\gamma-1}}{\Gamma(1+\gamma)}\left[\delta_x^2 U_i^{j+1} + \delta_x^2 U_i^j - 2\delta_x^2 U_i^{j+\frac{1}{2}}\right]\right.$$
$$+ K_\gamma \left[\frac{\partial^{1-\gamma}}{\partial t^{1-\gamma}}\delta_x^2 U\Big|_{ML1,i}^{j+\frac{1}{2}} - K_\gamma \left[\frac{\partial^{1-\gamma}}{\partial t^{1-\gamma}}\frac{\partial^2 U}{\partial x^2}\Big|_i^{j+\frac{1}{2}} - \frac{\Delta x^2}{4\Delta t}\left[\delta_x^2 U_i^{j+1} - \delta_x^2 U_i^j\right] + \frac{1}{2}\left[f_{i-\frac{1}{2}}^{j+\frac{1}{2}} + f_{i+\frac{1}{2}}^{j+\frac{1}{2}}\right]\right., \tag{23}$$

where $f_i^j = f(x_i, t_j)$ is the numerical approximation of the source term and

$$\delta_x^2 U_i^j = \frac{U_{i+1}^j - 2U_i^j + U_{i-1}^j}{\Delta x^2}. \tag{24}$$

Taking the Taylor series expansion around the point $(x_i, t_{j+\frac{1}{2}})$, Eq. (23) becomes

$$\left[\frac{\partial U}{\partial t}\Big|_i^{j+\frac{1}{2}} = K_\gamma \left[\frac{\partial^{1-\gamma}}{\partial t^{1-\gamma}}\left(\frac{\partial^2 U}{\partial x^2}\right)\Big|_i^{j+\frac{1}{2}} + f(x_i, t_{j+\frac{1}{2}}) + O(\Delta t^2) + O(\Delta x^2)\right.$$
$$\left. + K_\gamma \left[\left[\frac{\partial^{1-\gamma}}{\partial t^{1-\gamma}}\left(\frac{\partial^2 U}{\partial x^2}\right)\Big|_{ML1,i}^{j+\frac{1}{2}} - \left[\frac{\partial^{1-\gamma}}{\partial t^{1-\gamma}}\left(\frac{\partial^2 U}{\partial x^2}\right)\Big|_i^{j+\frac{1}{2}}\right]\right.\right. \tag{25}$$

where we note the term

$$\left[\frac{\partial^{1-\gamma}}{\partial t^{1-\gamma}}\left(\frac{\partial^2 U}{\partial x^2}\right)\Big|_{ML1,i}^{j+\frac{1}{2}} - \left[\frac{\partial^{1-\gamma}}{\partial t^{1-\gamma}}\left(\frac{\partial^2 U}{\partial x^2}\right)\Big|_i^{j+\frac{1}{2}}\right.\right. \tag{26}$$

is $O(\Delta t^{1+\gamma})$ as given in [34]. We then obtain

$$\left[\frac{\partial U}{\partial t}\Big|_i^{j+\frac{1}{2}} = K_\gamma \left[\frac{\partial^{1-\gamma}}{\partial t^{1-\gamma}}\left(\frac{\partial^2 U}{\partial x^2}\right)\Big|_i^{j+\frac{1}{2}} + f(x_i, t_{j+\frac{1}{2}}) + R_i^{j+1}\right.\right. \tag{27}$$

where the truncation error is

$$R_i^{j+1} = O(\Delta t^{1+\gamma} + \Delta x^2)\ , \tag{28}$$

for $i = 1, 2, \ldots, N$ and $j = 1, 2, \ldots, M$. Since i, j are finite, then there is a positive constant c_1 for all i, j such that

$$|R_i^{j+1}| \leq c_1(\Delta t^{1+\gamma} + \Delta x^2). \tag{29}$$

We then find the truncation error is of order $1+\gamma$ in time and second order in space. The numerical approximation for the fractional diffusion equation is consistent, since the truncation approaches zero as $\Delta t \to 0$ and $\Delta x \to 0$.

4. Stability analysis of the numerical method

In this section we investigate the local stability of the KBML1 numerical scheme in Eq. (21) using Von Neumann stability analysis. Now we let the error

$$E_i^j = U_i^j - u_i^j \tag{30}$$

where $i = 1, 2, \ldots, N$ and $j = 0, 1, 2, \ldots, M$ and so the error satisfies Eq. (21). To investigate the stability by Von Neumann stability analysis, we let

$$E_i^j = \xi_j e^{i' q i \Delta x}, \tag{31}$$

where $q = 2\pi l/L$ is a real spatial wave number and i' is the imaginary number, $i' = \sqrt{-1}$. From Eq. (21) we have

$$\begin{aligned} &\Delta x^2 \delta_x^2 U_i^{j+1} + 4U_i^{j+1} = \Delta x^2 \delta_x^2 U_i^j + 4U_i^j + 2\Delta t \left[f_{i-\frac{1}{2}}^{j+\frac{1}{2}} + f_{i+\frac{1}{2}}^{j+\frac{1}{2}} \right] \\ &+ \frac{4D\Delta t^\gamma}{\Gamma(1+\gamma)} \left\{ \beta_j(\gamma) \delta_x^2 U_i^0 + \left(\frac{1}{2}\right)^\gamma \left(\delta_x^2 U_i^{j+1} - \delta_x^2 U_i^j \right) + \sum_{k=1}^{j} \mu_{j-k}(\gamma) \left[\delta_x^2 U_i^k - \delta_x^2 U_i^{k-1} \right] \right\}. \end{aligned} \tag{32}$$

Subtracting Eq. (21) from Eq. (32), gives

$$\begin{aligned} &\Delta x^2 \delta_x^2 E_i^{j+1} + 4E_i^{j+1} = \Delta x^2 \delta_x^2 E_i^j + 4E_i^j \\ &+ \frac{4D\Delta t^\gamma}{\Gamma(1+\gamma)} \left\{ \beta_j(\gamma) \delta_x^2 E_i^0 + \left(\frac{1}{2}\right)^\gamma \left(\delta_x^2 E_i^{j+1} - \delta_x^2 E_i^j \right) + \sum_{k=1}^{j} \mu_{j-k}(\gamma) \left[\delta_x^2 E_i^k - \delta_x^2 E_i^{k-1} \right] \right\}. \end{aligned} \tag{33}$$

Using Eq. (31) in (33), we then obtain the recurrence relation

$$\xi_{j+1} = \xi_j - \lambda_q \left\{ \beta_j(\gamma) \xi_0 + \sum_{k=1}^{j} \mu_{j-k}(\gamma) \left[\xi_k - \xi_{k-1} \right] \right\}, \tag{34}$$

with

$$\lambda_q = \frac{V_q d}{1 - V_q + V_q \left(\frac{1}{2}\right)^\gamma d}, \quad \text{where} \quad V_q = \sin^2 \left(\frac{q\Delta x}{2} \right). \tag{35}$$

For $j \geq 1$, Eq. (34) becomes

$$\xi_{j+1} = \left[1 - \lambda_q \mu_0(\gamma) \right] \xi_j - \lambda_q \left\{ \alpha_j(\gamma) \xi_0 + \sum_{k=1}^{j-1} \omega_{j-k}(\gamma) \xi_k \right\} \tag{36}$$

with the weights

$$\alpha_j(\gamma) = \beta_j(\gamma) - \mu_{j-1}, \quad \text{and} \quad \omega_j(\gamma) = \mu_j - \mu_{j-1} \tag{37}$$

where $\beta_j(\gamma)$ and μ_j are as defined earlier in Eq. (11). We now consider three lemmas which will aid in showing the stability and convergence of our numerical method.

Lemma 4.1. Given $0 < \gamma \leq 1$ and $0 \leq V_q d < \infty$ then the parameter λ_q given in Eq (35) is bounded by $0 \leq \lambda_q \leq 2^\gamma$.

Proof. From Eq. (35), the term λ_q can be rewritten as

$$\lambda_q = \frac{1}{\frac{1-V_q}{V_q d} + \left(\frac{1}{2}\right)^\gamma}. \tag{38}$$

For $0 < V_q \leq 1$ and $0 < V_q d < \infty$, we then have $0 < \frac{1-V_q}{V_q d} < \infty$. Consequently, we have the bound $0 \leq \lambda_q \leq 2^\gamma$. □

Lemma 4.2. (adapted from [37]) Let $a_j = \left(j + \frac{1}{2}\right)^\gamma - \left(j - \frac{1}{2}\right)^\gamma$, where $j \geq 1$ and $0 < \gamma < 1$ then $a_j > 0$ and $a_j > a_{j+1}$.

Proof. Let $f_1(y) = \left(y - \frac{1}{2}\right)^\gamma$ and $f_2(y) = \left(y + \frac{1}{2}\right)^\gamma - \left(y - \frac{1}{2}\right)^\gamma$. For $y > 0$ it can be seen that $f_1(y)$ is a monotonically increasing function of y and $f_2(y)$ is a monotonically decreasing function of y. Thus $a_j > 0$ and $a_j > a_{j+1}$. □

Lemma 4.3. The coefficients $\alpha_j(\gamma)$ and $\omega_j(\gamma)$ defined in Eq. (37) for $j \geq 1$ satisfy $\alpha_j(\gamma) < 0$ and $\omega_j(\gamma) < 0$.

Proof. First we apply the binomial expansion to $\left(j - \frac{1}{2}\right)^\gamma$, then $\alpha_j(\gamma)$ becomes

$$\alpha_j(\gamma) = \sum_{n=2}^{\infty} \binom{\gamma}{n} (-1)^n \left(j + \frac{1}{2}\right)^{\gamma-n}. \tag{39}$$

After using the result in Appendix A, we then find

$$\alpha_j(\gamma) = \sum_{n=2}^{\infty} \frac{\gamma\Gamma(n-\gamma)}{n!\Gamma(1-\gamma)} (-1)^{2n-1} \left(j + \frac{1}{2}\right)^{\gamma-n} = -\sum_{n=2}^{\infty} \frac{\gamma\Gamma(n-\gamma)}{n!\Gamma(1-\gamma)} \left(j + \frac{1}{2}\right)^{\gamma-n} < 0 \tag{40}$$

since $n \geq 2$ and $0 < \gamma \leq 1$, the term $\frac{\gamma\Gamma(n-\gamma)}{(n)!\Gamma(1-\gamma)} > 0$, and the Gamma function is positive for positive arguments. By result (2) of Lemma 4.2 $\omega_j(\gamma) = a_{j+1} - a_j < a_j - a_j < 0$ then $\omega_j(\gamma) < 0$. Hence results (1) and (2) hold for $0 < \gamma < 1$. □

Proposition 4.4. Let ξ_j, where $j = 1, 2, ..., M$ be the solution of Eq. (34), then we have

$$| \xi_j | < | \xi_0 | \tag{41}$$

if $0 \leq \lambda_q \leq \min\left(2^\gamma, \frac{1}{\mu_0}\right)$ and $0 < \gamma < 1$.

Proof. We use mathematical induction method to prove Eq. (41). For simplicity we assume $\xi_0 > 0$. The case $\xi_0 < 0$ can be handled in analogous manner to the method below. For the case $j = 0$ in Eq. (34), we have

$$\xi_1 = \left(1 - \lambda_q \gamma \left(\frac{1}{2}\right)^{\gamma-1}\right) \xi_0. \tag{42}$$

We note $-1 < 1 - \lambda_q \gamma \left(\frac{1}{2}\right)^{\gamma-1} < 1$ since $0 \leq \lambda_q \leq 2^\gamma < 2^\gamma/\gamma$, then for $0 < \gamma < 1$ we have

$$-\xi_0 < \xi_1 < \xi_0, \text{ or } \qquad | \xi_1 | < | \xi_0 | \tag{43}$$

and so Eq. (41) is true for $j = 0$. We now assume, for some $k \in \mathbb{N}$, that

$$-\xi_0 < \xi_n < \xi_0, \text{ for } n = 1, 2, \ldots, k \tag{44}$$

and then we need to show that

$$-\xi_0 < \xi_{k+1} < \xi_0. \tag{45}$$

From Eq. (36) we have

$$\xi_{k+1} = [1 - \lambda_q \mu_0] \xi_k - \lambda_q \left\{ \alpha_k(\gamma) \xi_0 + \sum_{l=1}^{k-1} \omega_{k-l}(\gamma) \xi_l \right\} . \tag{46}$$

Note by using Lemma 4.3, we have $-\omega_{j-k}(\gamma) \geq 0$ and $-\alpha_k(\gamma) \geq 0$. We then consider cases, given $0 < \gamma < 1$ and $0 \leq \lambda_q \leq 2^\gamma$. The two cases depend upon the sign of the first term in Eq. (46).

The first case occurs if $(1 - \lambda_q \mu_0) > 0$, we have using Eqs. (44) and (46)

$$\xi_{k+1} \leq \left(1 - \lambda_q \mu_0 + \lambda_q \left(-\alpha_k(\gamma)\right) + \lambda_q \sum_{l=1}^{k-1} \left(-\omega_{k-l}(\gamma)\right)\right) \xi_0. \tag{47}$$

Evaluating the summation and using Eq. (37), we find

$$\xi_{k+1} \leq \left(1 - \frac{\lambda_q \gamma}{\left(k + \frac{1}{2}\right)^{1-\gamma}}\right) \xi_0 \leq \xi_0. \tag{48}$$

Likewise it can be shown $\xi_{k+1} \geq -\xi_0$, and so

$$-\xi_0 \leq \xi_{k+1} \leq \xi_0 \quad \text{or} \quad |\xi_{k+1}| \leq |\xi_0|. \tag{49}$$

Hence if $0 \leq \lambda_q \leq 2^\gamma$ and $(1 - \lambda_q \mu_0) > 0$ then Eq. (41) is satisfied for all $k \in \mathbb{N}$. Hence the numerical method is stable if $0 < \lambda_q < 2^\gamma$ and $1 - \lambda_q \mu_0 > 0$.
The second case occurs if $(1 - \lambda_q \mu_0) < 0$ and using a similar approach we have

$$-\rho(\gamma, k, \lambda_q)\xi_0 \leq \xi_{k+1} \leq \rho(\gamma, k, \lambda_q)\xi_0 \tag{50}$$

where

$$\rho(\gamma, k, \lambda_q) = 2\lambda_q \mu_0 - 1 - \lambda_q \gamma \left(k + \frac{1}{2}\right)^{\gamma - 1} \quad . \tag{51}$$

Unlike the first case, the value of $\rho(\gamma, k, \lambda_q)$ is not bounded by 1 for all values of λ_q, k and γ. As a result we cannot conclude from this analysis that the method is stable. However these bounds found are only estimates of the lower and upper bounds on the actual values of ξ_k and the actual values of ξ_k may be indeed still satisfy Proposition 4.4. In the next section we demonstrate the method is stable by evaluating the solution of the recurrence relationship in Eq. (46) numerically. Note if $\gamma = 1$ the solution of Eq. (46) is

$$\xi_k = (1 - \lambda_q)^k \xi_0 \ , \tag{52}$$

which is bounded if $0 \leq \lambda_q \leq 2$ for both cases. Langlands and Henry [22] found the same equation as Eq. (52) in the standard diffusion case ($\gamma = 1$). However in their case they found that the solution did not oscillate since their value of the parameter λ_q only had a range from 0 to 1. □

4.1. Numerical solution of the recurrence relationship

In this section we investigate the solution of the recurrence relationship in Eq. (46) by numerical evaluation for both cases. For the second case the value of the fractional exponent γ lies in the range $\log_3 2 \leq \gamma \leq 1$ where $\gamma = \log_3 2$ is the γ value at the intersection of $\lambda_q = 2^\gamma$ and $\lambda_q = 1/\mu_0$ curves. These results are shown in Fig. 1 for (a) $\lambda_q = 1/\mu_0$ and (b) $\lambda_q = 2^\gamma$, for $j = 0, \ldots, 5$ for varying γ. We see from Fig. 1(a) that the value of ξ_j/ξ_0 decays quickly to zero but does undergo some initial oscillation. Meanwhile in Fig. 1(b) we see the values of ξ_j/ξ_0 also oscillates but decays to zero more slowly if $0 < \gamma < 1$. We see similar behavior when we choose $\lambda_q = 2^{\log_3 2}$ as shown in

Fig. 2(a). Note that in the case of $\gamma = 1$, we have the solution $\xi_j/\xi_0 = (1 - \lambda_q)^j$ which for $\lambda_q = 2$ will oscillate between -1 and 1 as shown in Fig. 1(b) by the red dashed line. Whilst for $\gamma = 0$ the solution is $\xi_j/\xi_0 = 1$ as shown in Fig. 2(b) by the blue dashed line.

We also show results for the first case when $\lambda_q = 1$ and for various values of the fractional exponent γ in the range $0 < \gamma \leq 1$ in Fig. 2(b). We see the solution decays to zero but does not oscillate as in the second case. We note in Proposition 4.4 the difficulty we had in proving the stability for the second case is due to the oscillation. The oscillations do not occur for the first case and so we did not have the same issue. The results in Figs. 1 and 2 demonstrate this method is locally stable for both cases as the values of ξ_j/ξ_0 does not grow but instead remains bounded between -1 and 1.

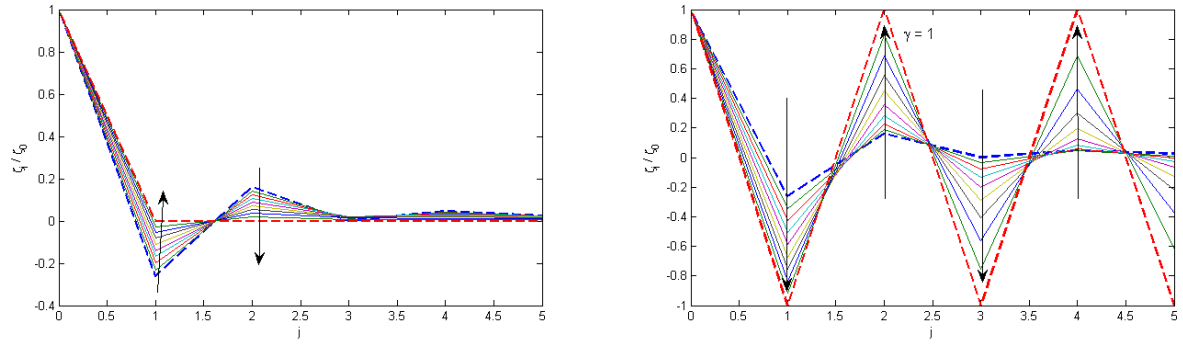

(a) (b)

Figure 1: In the second case, the predictions from Eq. (46) with $\xi_0 = 1$ for various γ is shown (a) for $\lambda_q = \frac{1}{\mu_0}$ and (b) for $\lambda_q = 2^\gamma$, for $j = 1, \ldots, 5$ and $\log_3 2 \leq \gamma \leq 1$. The ratios ξ_j/ξ_0 are bounded above by 1 and below by -1 and decay to zero for $0 < \gamma < 1$. Arrows show the direction of increasing γ.

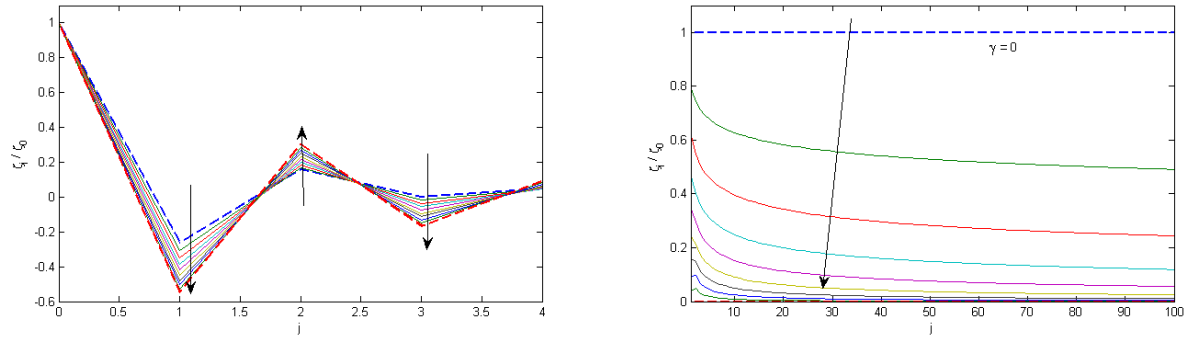

(a) (b)

Figure 2: The predictions from Eq. (46) with $\zeta_0 = 1$ for various γ is shown for (a) the second case with $\lambda_q = 2^{\log_3 2}$, j=1,. . . , 4 and $\log_3 2 \leq \gamma \leq 1$, and for (b) the first case with $\lambda_q = 1$, $j = 1, \ldots, 100$ and $0 < \gamma \leq 1$. The magnitude of the ratios remains less than 1 for $0 < \gamma < 1$. Arrows show the direction of increasing γ.

5. Convergence of the numerical method

In this section the convergence of the numerical methods given by Equations (21) is considered. We follow the approach as in [38], we define the following grid functions

$$E^j(x) = \begin{cases} E_i^j & \text{if } x \in \left(x_{i-\frac{1}{2}}, x_{i+\frac{1}{2}}\right], \; i = 1, 2, \ldots, N \\ 0 & \text{if } x \in \left[0, \frac{\Delta x}{2}\right] \bigcup \left(L - \frac{\Delta x}{2}, L\right], \end{cases} \tag{53}$$

and

$$R^j(x) = \begin{cases} R_i^j & \text{if } x \in \left(x_{i-\frac{1}{2}}, x_{i+\frac{1}{2}}\right], \; i = 1, 2, \ldots, N \\ 0 & \text{if } x \in \left[0, \frac{\Delta x}{2}\right] \bigcup \left(L - \frac{\Delta x}{2}, L\right] \end{cases} \tag{54}$$

where $i = 1, 2, \ldots, N$. Then expanding E_i^j and R_i^j in Fourier series we have

$$E^j(x) = \sum_{l=-\infty}^{\infty} \xi_j(l) e^{i' 2\pi l x / L}, \text{ and } R^j(x) = \sum_{l=-\infty}^{\infty} \eta_j(l) e^{i' 2\pi l x / L}, \text{ for } j = 0, 1, 2, \ldots, M, \tag{55}$$

where

$$\xi_j(l) = \frac{1}{L} \int_0^L E^j(x) e^{-i' 2\pi l x / L} dx, \qquad \text{and} \qquad \eta_j(l) = \frac{1}{L} \int_0^L R^j(x) e^{-i' 2\pi l x / L} dx. \tag{56}$$

Next we applied the Parseval identity [39, 40], we then have

$$\|E^j\|_2 = \left(\sum_{i=1}^{N-1} \Delta x |E_i^j|^2\right)^{\frac{1}{2}} = \left(\sum_{l=-\infty}^{\infty} |\xi_j(l)|^2\right)^{\frac{1}{2}}, \qquad j = 0, 1, 2, \ldots, M \tag{57}$$

and

$$\|R^j\|_2 = \left(\sum_{i=1}^{N-1} \Delta x |R_i^j|^2\right)^{\frac{1}{2}} = \left(\sum_{l=-\infty}^{\infty} |\eta_j(l)|^2\right)^{\frac{1}{2}}, \qquad j = 0, 1, 2, \ldots, M. \tag{58}$$

Now we assume that

$$R_i^j = \eta_j e^{i' q i \Delta x}, \tag{59}$$

where $q = 2\pi l/L$ is a real spatial wave number and i' is the imaginary number, $i' = \sqrt{-1}$.

From Eq. (30) we note that $E^0 = 0$, which satisfies the equation

$$\xi_0 = \xi_0(l) = 0. \tag{60}$$

By the convergence of the series on the right hand side (58) there is a positive constant c_j such that

$$|\eta_j| \equiv |\eta_j(l)| \leq c_j |\eta_1| \equiv c_j |\eta_1(l)|, \qquad j = 1, 2, \ldots, M. \tag{61}$$

We then obtain

$$|\eta_j| \leq c |\eta_1(l)|, \qquad j = 1, 2, \ldots, M, \tag{62}$$

where $c = \max_{1 \leq j \leq M}\{c_j\}$.

We will discuss the convergence of the KBML1 scheme, similar to Eq. (33) we have

$$\begin{aligned} &\Delta x^2 \delta_x^2 E_i^{j+1} + 4E_i^{j+1} = \Delta x^2 \delta_x^2 E_i^j + 4E_i^j + 4\Delta t R_i^{j+1} \\ &+ \frac{4D\Delta t^\gamma}{\Gamma(1+\gamma)} \left\{ \beta_j(\gamma) \delta_x^2 E_i^0 + \left(\frac{1}{2}\right)^\gamma \left(\delta_x^2 E_i^{j+1} - \delta_x^2 E_i^j\right) + \sum_{k=1}^{j} \mu_{j-k}(\gamma) \left[\delta_x^2 E_i^k - \delta_x^2 E_i^{k-1}\right] \right\}. \end{aligned} \tag{63}$$

Using Eq. (59) in (63), we then obtain the recurrence relation

$$\xi_{j+1} = \xi_j - \lambda_q \left\{ \beta_j(\gamma) \xi_0 + \sum_{k=1}^{j} \mu_{j-k}(\gamma) \left[\xi_k - \xi_{k-1}\right] \right\} + \frac{\Delta t \eta_{j+1}}{1 - V_q + V_q \left(\frac{1}{2}\right)^\gamma d}, \tag{64}$$

where λ_q and V_q are given in Eq. (35), and d is as defined in Eq. (22). When $j \geq 1$, Eq. (64) can be rewritten as

$$\xi_{j+1} = [1 - \lambda_q \mu_0(\gamma)]\, \xi_j - \lambda_q \left\{ \alpha_j(\gamma)\xi_0 + \sum_{k=1}^{j-1} \omega_{j-k}(\gamma)\xi_k \right\} + \frac{\Delta t \eta_{j+1}}{1 - V_q + dV_q \left(\frac{1}{2}\right)^\gamma} \tag{65}$$

where the weights $\alpha_j(\gamma)$ and $\omega_j(\gamma)$ are given in Eq. (37).

Proposition 5.1. Let ξ_j be the solution of Eq. (64). Then there exists a positive constant c_2 such that

$$|\xi_j| \leq c_2 j \Delta t |\eta_1|, \qquad j = 1, 2, \ldots, M, \tag{66}$$

if $0 \leq \lambda_q \leq \min(1/\mu_0(\gamma), 2^\gamma)$ and $0 < \gamma \leq 1$.

Proof. From Eqs. (29) and (58), we obtain

$$\|R^j\|_2 \leq c_2 \sqrt{N\Delta x}(\Delta t^{1+\gamma} + \Delta x^2) = c_2 \sqrt{L}(\Delta t^{1+\gamma} + \Delta x^2), \tag{67}$$

where $j = 1, 2, \ldots, M$. We use mathematical induction to prove the relation in Eq. (66). We first consider the case $j = 0$, from Eq. (64) and using Eq. (60), we have

$$\xi_1 = \frac{\Delta t}{1 - V_q + V_q d \left(\frac{1}{2}\right)^\gamma} \eta_1 \tag{68}$$

since $0 \leq V_q \leq 1$ and $d > 0$, we obtain

$$|\xi_1| \leq \frac{\Delta t}{1 - V_q + V_q d \left(\frac{1}{2}\right)^\gamma} |\eta_1| \leq \Delta t |\eta_1| \leq c_2 \Delta t |\eta_1|. \tag{69}$$

Suppose that

$$|\xi_n| \leq c_2 n \Delta t |\eta_1|, \qquad n = 1, 2, \ldots, k. \tag{70}$$

For $0 < \gamma < 1$ and $dV_q > 0$, from Eq. (65), we have

$$|\xi_{k+1}| \leq |1 - \lambda_q \mu_0(\gamma)|\, |\xi_k| + \lambda_q\, |-\alpha_k(\gamma)|\, |\xi_0| + \lambda_q \sum_{l=1}^{k-1} |-\omega_{k-l}(\gamma)|\, |\xi_l| + \left| \frac{\Delta t \eta_{k+1}}{1 - V_q + V_q d \left(\frac{1}{2}\right)^\gamma} \right|. \tag{71}$$

Now using Eqs. (60) and (70) in Eq. (71), gives

$$|\xi_{k+1}| \leq c_2 \Delta t \left\{ |1 - \lambda_q \mu_0(\gamma)|\, k + \lambda_q \sum_{l=1}^{k-1} l\, |-\omega_{k-l}(\gamma)| + \left| \frac{1}{1 - V_q + V_q \left(\frac{1}{2}\right)^\gamma d} \right| \right\} |\eta_1|\,. \tag{72}$$

The sign of the first term $(1-\lambda_q\mu_0(\gamma))$ may be positive or negative. Also for $0<\gamma<1$ and $V_q d>0$, we note

$$0 \leq \frac{1}{1-V_q+V_q\left(\frac{1}{2}\right)^{\gamma} d} \leq 1. \tag{73}$$

By Lemma 4.3 the weights $\omega_j(\gamma)$ are negative then $-\omega_j(\gamma)>0$, we then evaluate the summation in Eq. (72) by

$$\sum_{l=1}^{k-1} l\left(-\omega_{k-l}(\gamma)\right) = k\mu_0(\gamma) - \left(k+\frac{1}{2}\right)^{\gamma} + \left(\frac{1}{2}\right)^{\gamma}. \tag{74}$$

We need to consider two cases.

Case 1 occurs if the first term satisfies $(1-\lambda_q\mu_0(\gamma)) \geq 0$. Using Eq. (74) in Eq. (72), we then have

$$|\xi_{k+1}| \leq c_2\Delta t\left[k+\frac{1}{1-V_q+V_q d\left(\frac{1}{2}\right)^{\gamma}}\right]|\eta_1| - c_2\Delta t\lambda_q\left[\left(k+\frac{1}{2}\right)^{\gamma} - \left(\frac{1}{2}\right)^{\gamma}\right]|\eta_1|. \tag{75}$$

Since for $0<\gamma\leq 1$ we have $\left(k+\frac{1}{2}\right)^{\gamma} - \left(\frac{1}{2}\right)^{\gamma} > 0$, and by using Eq. (73), we then conclude that

$$|\xi_{k+1}| \leq c_2\Delta t(k+1)|\eta_1|, \tag{76}$$

and hence Eq. (66) is satisfied. Therefore if $0\leq\lambda_q\leq 2^{\gamma}$ and $1-\lambda_q\mu_0(\gamma)\geq 0$ then Eq. (66) is satisfied for all $j\geq 0$. The proof of the proposition is completed for Case 1.

Case 2 occurs if the first term satisfies $1-\lambda_q\mu_0(\gamma)\leq 0$. From Lemma 4.1 we have $0\leq\lambda_q\leq 2^{\gamma}$ and $0<\gamma<1$, then using Eq. (74) in Eq. (72), we have

$$\begin{aligned}|\xi_{k+1}| &\leq c_2\Delta t\left\{\left[\lambda_q\mu_0(\gamma)-1\right]k + \lambda_q\left[k\mu_0(\gamma) - \left(k+\frac{1}{2}\right)^{\gamma} + \left(\frac{1}{2}\right)^{\gamma}\right] + \frac{1}{1-V_q+V_q d\left(\frac{1}{2}\right)^{\gamma}}\right\}|\eta_1| \\ &\leq c_2\Delta t(2^{\gamma+1}\mu_0(\gamma)k+1)|\eta_1|, \end{aligned} \tag{77}$$

since the term $0<2^{\gamma+1}\mu_0(\gamma)\leq 4$. We then conclude that for $n=k+1$

$$|\xi_{k+1}| \leq 4c_2\Delta t(k+1)|\eta_1|, \tag{78}$$

but this does not satisfy the assumption in Eq. (70) and so convergence in this case cannot be confirmed. □

Theorem 5.2. Let $u(x,t)\in U(\Omega)$ be the exact solution for the fractional subdiffusion equation. Then the numerical scheme given by Equations (21) is convergent with order $O(\Delta t^{1+\gamma})+O(\Delta x^2)$ if $\lambda_q=\min(1/\mu_0(\gamma), 2^{\gamma})$.

Proof. Using Eqs. (57) and (58) with Eq. (29) and Proposition 5.1, for $j\Delta t \leq T$, we then obtain

$$\|E^j\|_2 \leq c_2 \Delta t k \|R_1\| \leq c_1 c_2 j \Delta t \sqrt{L}(\Delta t^{1+\gamma} + \Delta x^2) \leq C(\Delta t^{1+\gamma} + \Delta x^2) \tag{79}$$

where $C = c_1 c_2 T\sqrt{L}$. □

6. Numerical examples

In this section we provide three examples of the implementation our Keller Box scheme on problems where the analytic solution is known. For each example we compare graphically the numerical predictions against the exact solution. We also verify the accuracy of the implicit scheme by computing the maximum norm of the error between the numerical estimate u_i^M and the exact solution $u(x_i, t_M)$ using the infinity norm

$$e_\infty(\Delta t, \Delta x) = \max_{1 \leq i \leq N} \mid u_i^M - u(x_i, t_M) \mid . \tag{80}$$

Numerical accuracy is tested for varying time and spatial steps, and for four different fractional exponents $\gamma = 0.1, 0.5, 0.9$, and 1. The approximate order of convergence in Δx, R_1, was estimated by computing

$$R_1 = \log_2 \left[e_\infty(\Delta t, 2\Delta x)/e_\infty(\Delta t, \Delta x) \right], \tag{81}$$

and the approximate order of convergence in Δt, R_2, was estimated by computing

$$R_2 = \log_2 \left[e_\infty(2\Delta t, \Delta x)/e_\infty(\Delta t, \Delta x) \right]. \tag{82}$$

Example 6.1. Consider the following fractional subdiffusion equation with a source term

$$\frac{\partial u}{\partial t} = K_\gamma \frac{\partial^{1-\gamma}}{\partial t^{1-\gamma}} \left(\frac{\partial^2 u}{\partial x^2} \right) + \sin(\pi x) \left[(2+\gamma) t^{1+\gamma} + \pi^2 \left(\frac{t^{\gamma-1}}{\Gamma(\gamma)} + \frac{\Gamma(3+\gamma) t^{1+2\gamma}}{\Gamma(2+2\gamma)} \right) \right], \tag{83}$$

with $0 < \gamma \leq 1$ and the initial and fixed boundary conditions

$$u(x,0) = \sin(\pi x), \qquad u(0,t) = 0, \quad u(1,t) = 0 \ . \tag{84}$$

The exact solution of Eq. (83) given the conditions Eq. (84) is

$$u(x,t) = \left(1 + t^{2+\gamma}\right) \sin(\pi x). \tag{85}$$

In Tables 1 and 2, we give the error and order of convergence estimates for this example. To estimate the convergence in space we kept Δt fixed at 10^{-3} whilst varying Δx. To estimate the

convergence in time we kept Δx fixed at 10^{-3} whilst varying Δt. From the results shown in Tables 1 and 2, by using KBML1 for Eq. (83), it can be seen that, the KBML1 scheme appears to be of order $O(\Delta x^2)$, and $O(\Delta t^{1+\gamma})$.

Table 1: Numerical accuracy in Δx applied to Eq. (83) with $\Delta t = 10^{-3}$ and R_1 is order of convergence.

	$\gamma = 0.1$		$\gamma = 0.5$		$\gamma = 0.9$		$\gamma = 1$	
Δx	$e_\infty(\Delta t, \Delta x)$	R_1	$e_\infty(\Delta t, \Delta x)$	R_1	$e_\infty(\Delta t, \Delta x)$	R_1	$e_\infty(\Delta t, \Delta x)$	R_1
1/2	1.65e–01	–	1.99e–01	–	1.75e–01	–	1.66e–01	–
1/4	3.21e–02	2.36	3.82e–02	2.38	3.17e–02	2.46	2.93e–02	2.50
1/8	7.54e–03	2.09	8.91e–03	2.10	7.26e–03	2.12	6.67e–03	2.13
1/16	1.88e–03	2.01	2.19e–03	2.02	1.78e–03	2.03	1.63e–03	2.03
1/32	4.89e–04	1.94	5.51e–04	1.99	4.43e–04	2.01	4.05e–04	2.01

Table 2: Numerical accuracy in Δt applied to Eq. (83) with $\Delta x = 10^{-3}$ and R_2 is order of convergence.

	$\gamma = 0.1$		$\gamma = 0.5$		$\gamma = 0.9$		$\gamma = 1$	
Δt	$e_\infty(\Delta t, \Delta x)$	R_2	$e_\infty(\Delta t, \Delta x)$	R_2	$e_\infty(\Delta t, \Delta x)$	R_2	$e_\infty(\Delta t, \Delta x)$	R_2
1/10	5.48e–03	–	9.26e–03	–	7.27e–03	–	6.99e–03	–
1/20	2.40e–03	1.19	3.00e–03	1.63	1.87e–03	1.96	1.75e–03	2.00
1/40	1.07e–03	1.16	9.90e–04	1.60	4.83e–04	1.96	4.38e–04	2.00
1/80	4.88e–04	1.14	3.32e–04	1.58	1.25e–04	1.95	1.10e–04	2.00
1/160	2.25e–04	1.12	1.13e–04	1.55	3.30e–05	1.94	2.80e–05	1.98

A comparison of the exact and numerical solution of Eq. (83), at the point $x = 0.5$ and for $0 < t \leq 1$ for the fractional exponents $\gamma = 0.1$, 0.5, and 0.9 with $\Delta t = 10^{-3}$, is shown in Fig. 3. We also show in Fig. 4 the comparison of the exact solution (shown as solid red lines) with the numerical solution (shown as blue dots), at the times $t = 0.25$, 0.50, 0.75, and 1.00 for $\gamma = 0.1$ and 0.9. It can be seen that from both Figs. 3 and 4, for $0 \leq \lambda_q \leq 1$, the approximate solution obtained from the KBML1 scheme, is in good agreement with the exact solution.

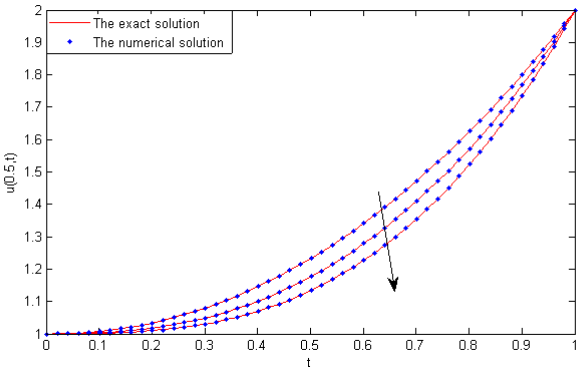

Figure 3: (Color online) A comparison of the exact solution (solid red lines) and the numerical solution (blue dots) for Eq. (83) at the point $x = 0.5$ and time $0 \leq t \leq 1$, for $\gamma = 0.1$, 0.5, and 0.9 with $\Delta t = 10^{-3}$. Note γ increases in the direction of arrow. (For interpretation of the references to color in this figure legend, the reader is referred to the web version of this article.)

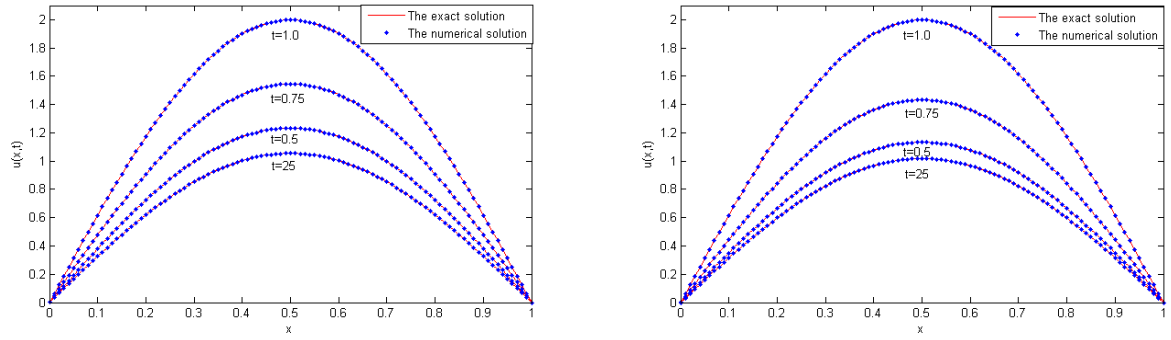

(a) (b)

Figure 4: (Color online) A comparison of the exact solution (solid red lines) and the numerical solution (blue dots) for Eq. (83) for (a) $\gamma = 0.1$ and (b) $\gamma = 0.9$ at the times $t = 0.25$, 0.50, 0.75, and 1.0 with $\Delta t = 10^{-3}$. (For interpretation of the references to color in this figure legend, the reader is referred to the web version of this article.)

We also investigate the stability in the case $1 < \lambda_q < 2^\gamma$ where the analysis was inconclusive. By calculating the relative error in the numerical solution, we can demonstrate the numerical solution is stable if the error decays with time. In Figs. 5 and 6 we show the relative error for the exponent values $\gamma = 0.6$, 0.7, 0.8, and 0.9 at the time $t = 5$ using increasingly larger time steps $\Delta t = 0.25$, 0.3125, 0.5, and 1. In Fig. 5, for $\gamma = 0.6$ and $\gamma = 0.7$, we have estimated the ranges of λ_q as $1.15 \leq \lambda_q \leq 1.41$ and $1.17 \leq \lambda_q \leq 1.51$ respectively. Likewise in Fig. 6 we have $1.16 \leq \lambda_q \leq 1.61$ for $\gamma = 0.8$ and $1.14 \leq \lambda_q \leq 1.73$ for $\gamma = 0.9$. We see the relative errors do indeed decay with time.

This indicates the solution is stable despite the large time steps chosen.

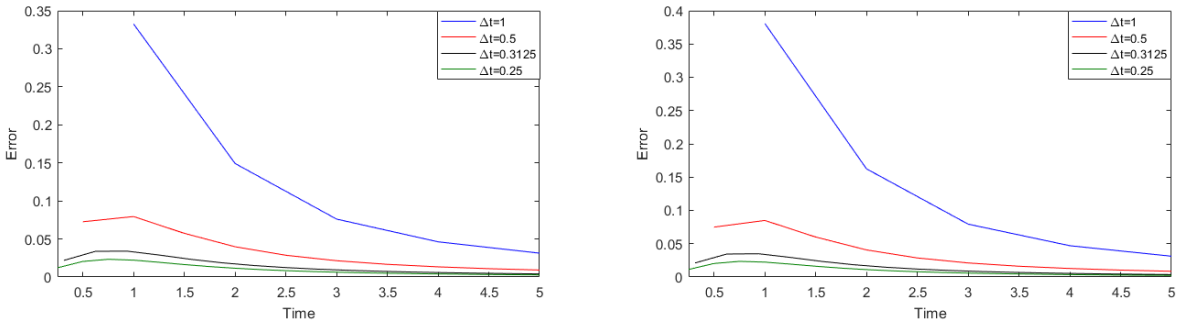

(a) (b)

Figure 5: (Color online) The relative error for the numerical solution Eq. (83) for (a) $\gamma = 0.6$ with $1.15 \leq \lambda_q \leq 1.41$ and (b) $\gamma = 0.7$ with $1.17 \leq \lambda_q \leq 1.51$ at time $t = 5$ and $\Delta t = 0.25, 0.3125, 0.5, 1$.

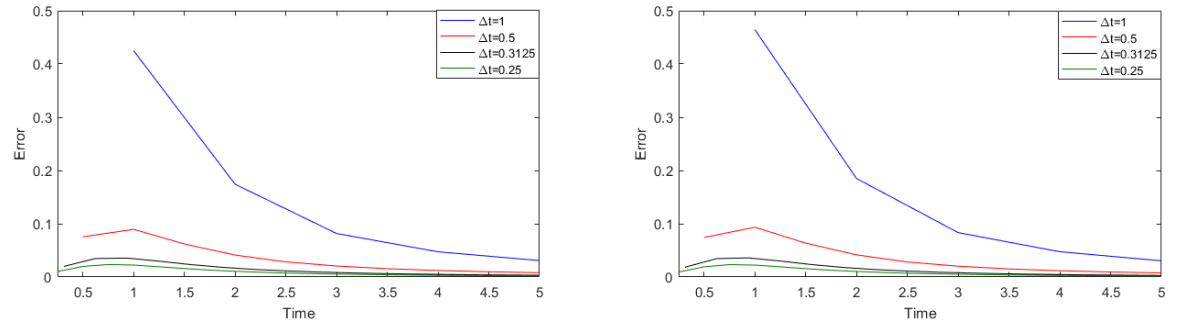

(a) (b)

Figure 6: (Color online) The relative error for the numerical solution Eq. (83) for (a) $\gamma = 0.8$ with $1.16 \leq \lambda_q \leq 1.61$ and (b) $\gamma = 0.9$ with $1.14 \leq \lambda_q \leq 1.73$ at the time $t = 5$ with $\Delta t = 0.25, 0.3125, 0.5, 1$.

Example 6.2. Consider the following fractional Subdiffusion equation with the source term

$$\frac{\partial u}{\partial t} = K_\gamma \frac{\partial^{1-\gamma}}{\partial t^{1-\gamma}} \left(\frac{\partial^2 u}{\partial x^2} \right) + (2+\gamma) e^x t^{1+\gamma} \left[1 - \frac{\Gamma(2+\gamma) t^\gamma}{\Gamma(2+2\gamma)} \right], \tag{86}$$

with $0 < \gamma \leq 1$ and the initial and fixed boundary conditions

$$u(x,0) = 0, \quad u(0,t) = t^{2+\gamma}, \quad u(1,t) = et^{2+\gamma}. \tag{87}$$

The exact solution of Eqs. (86) and (87) is

$$u(x,t) = e^x t^{2+\gamma}. \tag{88}$$

Error and order of convergence estimates for this example is shown in Tables 3 and 4. Similar to the previous example we estimate the convergence in space and time. We see the truncation order of the KBML1 scheme is of order $O(\Delta x^2)$ and $O(\Delta t^{1+\gamma})$.

Table 3: Numerical accuracy in Δx applied to Eq. (86) with $\Delta t = 10^{-3}$ and R_1 is order of convergence.

	$\gamma = 0.1$		$\gamma = 0.5$		$\gamma = 0.9$		$\gamma = 1$	
Δx	$e_\infty(\Delta t, \Delta x)$	R_1	$e_\infty(\Delta t, \Delta x)$	R_1	$e_\infty(\Delta t, \Delta x)$	R_1	$e_\infty(\Delta t, \Delta x)$	R_1
1/2	8.87e–03	–	1.21e–02	–	1.76e–02	–	1.95e–02	–
1/4	2.13e–03	2.06	2.87e–03	2.08	4.10e–03	2.11	4.52e–03	2.11
1/8	5.23e–04	2.03	7.07e–04	2.02	1.01e–03	2.02	1.11e–03	2.03
1/16	1.27e–04	2.05	1.76e–04	2.00	2.53e–04	1.99	2.79e–04	1.99
1/32	2.70e–05	2.23	4.30e–05	2.04	6.30e–05	2.00	7.00 e–05	2.00

Table 4: Numerical accuracy in Δt applied to Eq. (86) with $\Delta x = 10^{-3}$ and R_2 is order of convergence.

	$\gamma = 0.1$		$\gamma = 0.5$		$\gamma = 0.9$		$\gamma = 1$	
Δt	$e_\infty(\Delta t, \Delta x)$	R_2	$e_\infty(\Delta t, \Delta x)$	R_2	$e_\infty(\Delta t, \Delta x)$	R_2	$e_\infty(\Delta t, \Delta x)$	R_2
1/10	1.08e–03	–	1.67e–03	–	1.03e–03	–	8.96e–04	–
1/20	4.86e–04	1.16	5.61e–04	1.57	2.69e–04	1.94	2.24e–04	2.00
1/40	2.21e–04	1.14	1.91e–04	1.56	7.00e–05	1.94	5.60e–05	2.00
1/80	1.02e–04	1.12	6.50e–05	1.54	1.80e–05	1.94	1.40e–05	2.01
1/160	4.70e–05	1.11	2.30e–05	1.53	5.00e–06	1.95	3.00e–06	2.02

A comparison of the exact and numerical solution of Eq. (86) at the point $x = 0.5$, $0 \leq t \leq 1$, for $\gamma = 0.1$, 0.5, and 0.9 with $\Delta t = 10^{-3}$, is shown in Fig. 7. In Fig. 8 we also show the comparison of the exact solution (shown as solid red lines) with the numerical solution (shown as blue dots) at the times $t = 0.25$, 0.5, 0.75, and 1.00, and fractional exponents $\gamma = 0.1$ and 0.9. Again from both Figs. 7 and 8, for $0 \leq \lambda_q \leq 1$, we see the numerical estimates is in agreement with the exact solution.

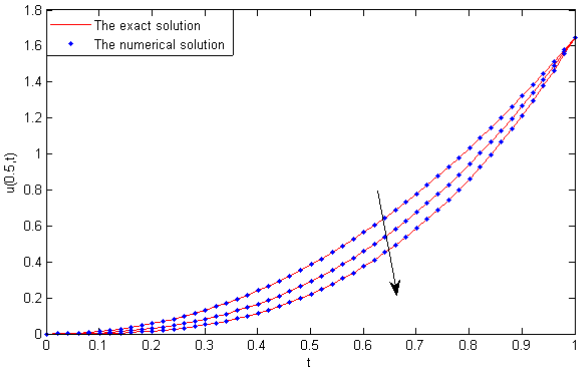

Figure 7: (Color online) A comparison of the exact solution (solid red lines) and the numerical solution (blue dots) for Eq. (86) at the point $x = 0.5$ and time $0 \leq t \leq 1$, for $\gamma = 0.1$, 0.5, and 0.9 with $\Delta t = 10^{-3}$. Note γ increases in the direction of arrow. (For interpretation of the references to color in this figure legend, the reader is referred to the web version of this article.)

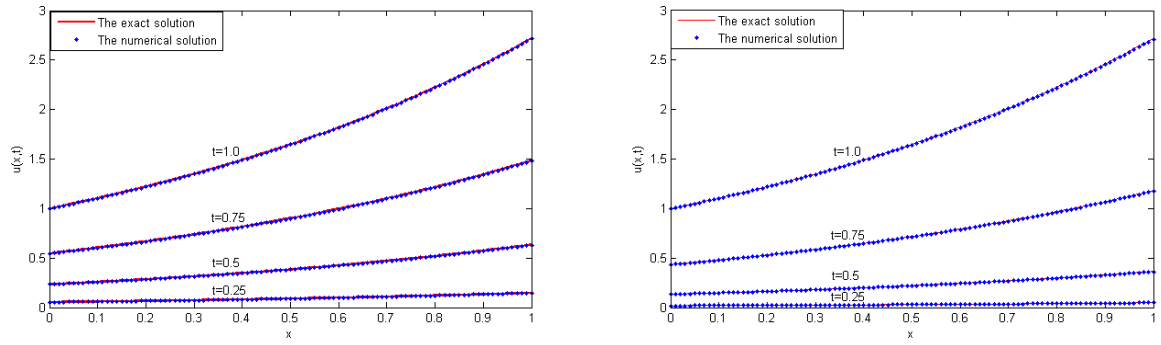

(a) (b)

Figure 8: (Color online) A comparison of the exact solution (solid red lines) and the numerical solution (blue dots) for Eq. (86) for (a) $\gamma = 0.1$ and (b) $\gamma = 0.9$ at the times $t = 0.25$, 0.50, 0.75, and 1.0 with $\Delta t = 10^{-3}$. (For interpretation of the references to color in this figure legend, the reader is referred to the web version of this article.)

In Figs. 9 and 10 we show again the relative error for the case $1 < \lambda_q < 2^{\gamma}$ at time $t = 5$ and $\Delta t = 1$, 0.5, 0.3125, 0.25. The estimated range of λ_q are $1.15 \leq \lambda_q \leq 1.41$ for $\gamma = 0.6$, $1.17 \leq \lambda_q \leq 1.51$ for $\gamma = 0.7$, $1.16 \leq \lambda_q \leq 1.61$ for $\gamma = 0.8$ and $1.14 \leq \lambda_q \leq 1.73$ for $\gamma = 0.9$. It is noted the relative errors for $\gamma = 0.9$ are largest initially for the case $\Delta t = 0.25$ compared to the other cases of γ. Again we see the relative errors decrease as time increases, and hence the numerical solution is stable.

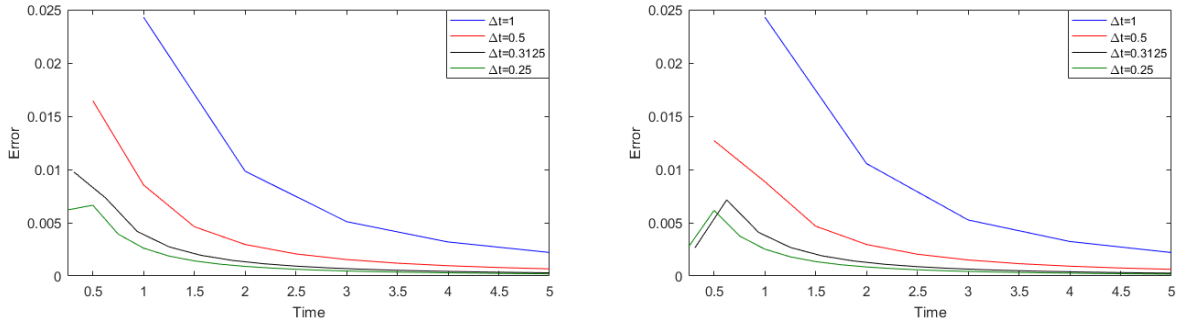

(a) (b)

Figure 9: (Color online) The relative error for the numerical solution Eq. (86), for (a) $\gamma = 0.6$ with $1.15 \leq \lambda_q \leq 1.41$ and (b) $\gamma = 0.7$ with $1.17 \leq \lambda_q \leq 1.51$ where time $t = 5$ and $\Delta t = 0.25, 0.3125, 0.5, 1$.

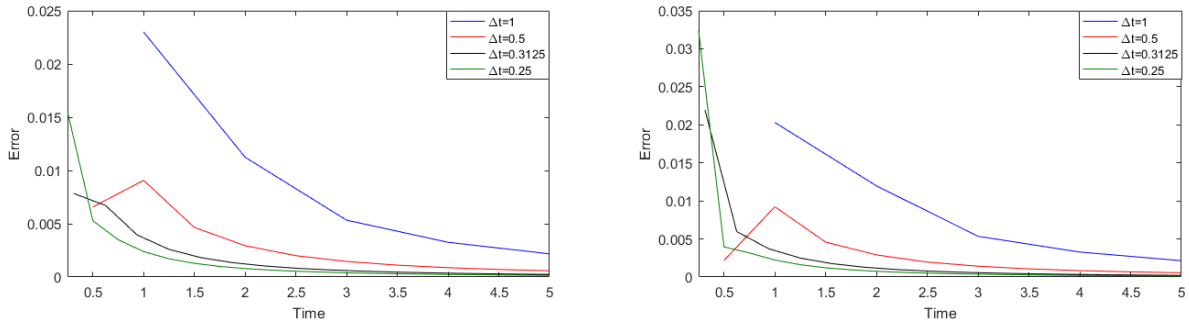

(a) (b)

Figure 10: (Color online) The relative error for the numerical solution Eq. (86), for (a) $\gamma = 0.8$ with $1.16 \leq \lambda_q \leq 1.61$ and (b) $\gamma = 0.9$ with $1.14 \leq \lambda_q \leq 1.73$ at time $t = 5$ and $\Delta t = 0.25, 0.3125, 0.5, 1$.

Example 6.3. Consider the following fractional differential equation

$$\frac{\partial u}{\partial t} = K_\gamma \frac{\partial^{1-\gamma}}{\partial t^{1-\gamma}} \left(\frac{\partial^2 u}{\partial x^2} \right) - \alpha u + f(x,t), \tag{89}$$

where

$$f(x,t) = e^x \left[x^2(1-x)^2 \left[(2+\gamma)t^{1+\gamma} + \alpha t^{2+\gamma} \right] - K_\gamma \left(2 - 8x + x^2 + 6x^3 + x^4 \right) \frac{\Gamma(3+\gamma) t^{1+2\gamma}}{\Gamma(2+2\gamma)} \right], \tag{90}$$

with $0 < \gamma \leq 1$ and the initial and fixed boundary conditions

$$u(x,0) = 0, \quad u(0,t) = 0, \quad u(1,t) = 0. \tag{91}$$

The exact solution of Eqs. (89) and (91) is

$$u(x,t) = e^x x^2 (1-x)^2 t^{2+\gamma}. \tag{92}$$

The error and order of convergence estimates found from applying the KBML1 scheme on Eq. (89) subject to Eq. (91). Again we estimate the convergence in space and time, the results shown in Tables 5 and 6. It can be seen that the KBML1 scheme appear to be of order $O(\Delta x^2)$ and $O(\Delta t^{1+\gamma})$.

Table 5: Numerical accuracy in Δx applied to Eq. (89) with $\Delta t = 10^{-3}$ and R_1 is order of convergence.

	$\gamma = 0.1$		$\gamma = 0.5$		$\gamma = 0.9$		$\gamma = 1$	
Δx	$e_\infty(\Delta t, \Delta x)$	R_1	$e_\infty(\Delta t, \Delta x)$	R_1	$e_\infty(\Delta t, \Delta x)$	R_1	$e_\infty(\Delta t, \Delta x)$	R_1
1/4	1.24e–02	–	1.17e–02	–	1.04e–02	–	1.00e–02	–
1/8	3.20e–03	1.96	2.97e–03	1.99	2.60e–03	2.01	2.47e–03	2.02
1/16	8.21e–04	1.96	7.49e–04	1.99	6.48e–04	2.00	6.16e–04	2.01
1/32	2.08e–04	1.98	1.89e–04	1.99	1.62e–04	2.00	1.54e–04	2.00
1/64	5.40e–05	1.95	4.80e–05	1.99	4.10e–05	2.00	3.80e–05	2.00

Table 6: Numerical accuracy in Δt applied to Eq. (89) with $\Delta x = 10^{-3}$ and R_2 is order of convergence.

	$\gamma = 0.1$		$\gamma = 0.5$		$\gamma = 0.9$		$\gamma = 1$	
Δt	$e_\infty(\Delta t, \Delta x)$	R_2	$e_\infty(\Delta t, \Delta x)$	R_2	$e_\infty(\Delta t, \Delta x)$	R_2	$e_\infty(\Delta t, \Delta x)$	R_2
1/10	5.85e–04	–	9.71e–04	–	7.78e–04	–	7.54e–04	–
1/20	2.52e–04	1.22	3.13e–04	1.64	2.00e–04	1.96	1.89e–04	2.00
1/40	1.12e–04	1.17	1.03e–04	1.61	5.20e–05	1.96	4.70e–05	2.00
1/80	5.10e–05	1.14	3.40e–05	1.58	1.30e–05	1.95	1.20e–05	1.99
1/160	2.30e–05	1.12	1.20e–05	1.55	4.00e–06	1.92	3.00e–06	1.96

In Fig. 12 we again show the comparison of the exact solution (shown as solid red lines) and the numerical estimate found using the KBML1 methods (shown as blue dots) at the times $t = 0.25$, 0.5, 0.75, and 1.00, with the fractional exponents $\gamma = 0.1$ and 0.9. We also show the comparison of the exact and numerical solution of Eq. (89) at the point $x = 0.5$, $0 \leq t \leq 1$, for $\gamma = 0.1$, 0.5, and 0.9 with $\Delta t = 10^{-3}$ in Fig. 11. Again from both Figs. 11 and 12, for $0 \leq \lambda_q \leq 1$, we see the numerical estimates is in agreement with the exact solution.

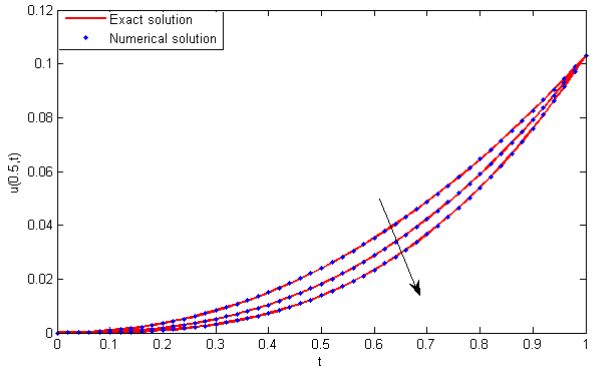

Figure 11: (Color online) A comparison of the exact solution (solid red lines) and the numerical solution (blue dots) for Eq. (89) at the point $x = 0.5$ and time $0 \leq t \leq 1$, for $\gamma = 0.1$, 0.5, and 0.9 with $\Delta t = 10^{-3}$. Note γ increases in the direction of arrow. (For interpretation of the references to color in this figure legend, the reader is referred to the web version of this article.)

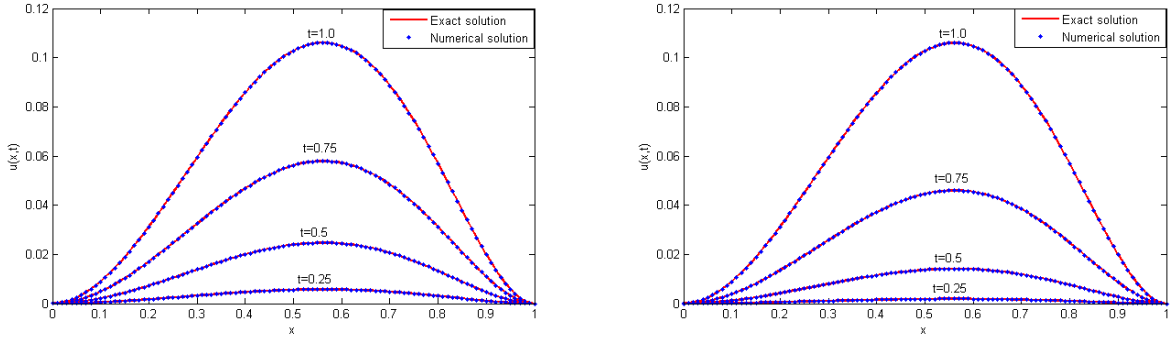

(a) (b)

Figure 12: (Color online) A comparison of the exact solution (solid red lines) and the numerical solution (blue dots) for Eq. (89) for (a) $\gamma = 0.1$ and (b) $\gamma = 0.9$ at the times $t = 0.25$, 0.50, 0.75, and 1.0 with $\Delta t = 10^{-3}$. (For interpretation of the references to color in this figure legend, the reader is referred to the web version of this article.)

In this example we also investigate the stability by evaluating the relative error in the numerical predictions in the case $1 < \lambda_q < 2^{\gamma}$. The relative errors are shown in Figs. 13 and 14 for $\gamma = 0.6$, 0.7, 0.8 and 0.9 at time $t = 5$ with $\Delta t = 0.25$, 0.3125, 0.5, 1. The estimated ranges of λ_q in these cases are $1.41 \leq \lambda_q \leq 1.49$ for $\gamma = 0.6$, $1.48 \leq \lambda_q \leq 1.59$ for $\gamma = 0.7$, $1.55 \leq \lambda_q \leq 1.71$ for $\gamma = 0.8$ and $1.61 \leq \lambda_q \leq 1.83$ for $\gamma = 0.9$. Again, it can be seen that the relative errors decrease as time progresses despite the relatively large time steps chosen. This demonstrates again, for this example, that the method is stable.

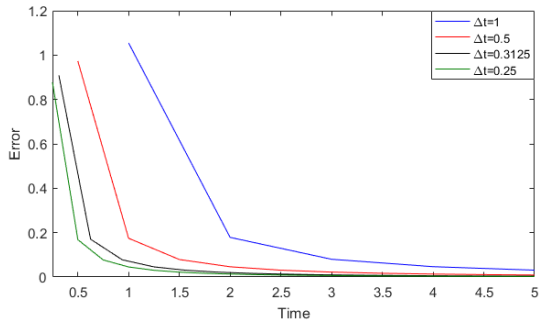

(a)

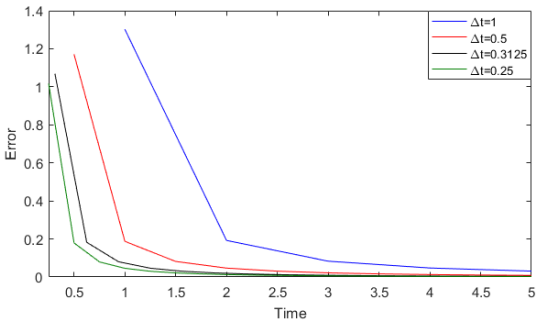

(b)

Figure 13: (Color online) The relative error for the numerical solution Eq. (89), for (a) $\gamma = 0.6$ with $1.41 \leq \lambda_q \leq 1.49$ and (b) $\gamma = 0.7$ with $1.48 \leq \lambda_q \leq 1.59$ at the time $t = 5$ and $\Delta t = 0.25, 0.3125, 0.5, 1$.

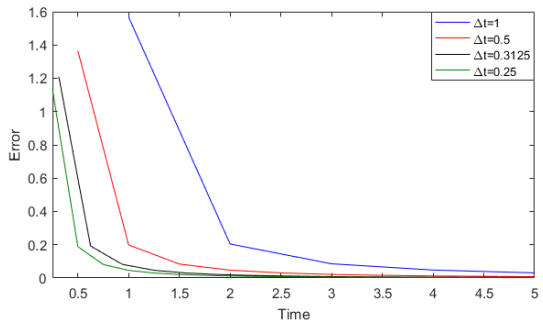

(a)

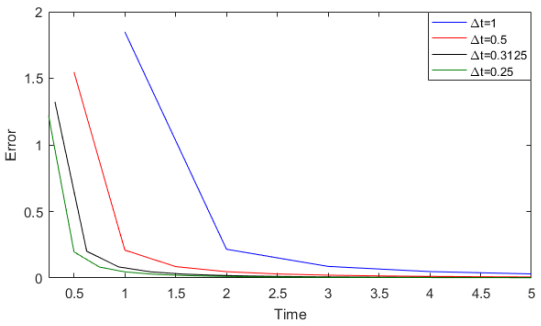

(b)

Figure 14: (Color online) The relative error for the numerical solution Eq. (89), for (a) $\gamma = 0.8$ with $1.55 \leq \lambda_q \leq 1.71$ and (b) $\gamma = 0.9$ with $1.61 \leq \lambda_q \leq 1.83$ at the time $t = 5$ and $\Delta t = 0.25, 0.3125, 0.5, 1$.

7. Conclusion

In this work, we constructed a Keller Box numerical scheme, KBML1, for the solution of fractional subdiffusion equation. A modification of L1 scheme (ML1) was used to estimate the Riemann–Liouville fractional derivative at the time $t_{j+\frac{1}{2}}$. The accuracy of KBML1 was found to be order $1+\gamma$ in time and second order in space. We proved the stability and convergence of the KBML1 method in the case where $0 < \lambda_q < \min(\frac{1}{\mu_0}, 2^\gamma)$ and $0 < \gamma \leq 1$. We also demonstrated the method is also stable numerically in the case where $\frac{1}{\mu_0} < \lambda_q \leq 2^\gamma$ and $\log_3 2 \leq \gamma \leq 1$ by using the Von-Neumann stability analysis and using the full numerical solution. The convergence orders were confirmed when the scheme was applied to three test examples. This method can be used

for more general equations where we cannot rewrite fractional partial differential equation with a Caputo derivative on the left such as the nonlinear reaction subdiffusion models of Angstmann et al. [41]. This will be a subject of another article in preparation.

Acknowledgments

This work was supported by the Australian Research Council (ARC DP130100595).

Appendix A. Binomial coefficient identity

Using the definition of the binomial coefficient, we can rewrite the coefficient in terms of the Gamma function

$$\begin{pmatrix} \gamma \\ k \end{pmatrix} = (-1)^k \binom{k}{k-\gamma-1} = \frac{\gamma\Gamma(k-\gamma)}{\Gamma(1-\gamma)} \, \frac{(-1)^{k-1}}{k!} \, . \tag{A.1}$$

[1] H. B. Keller, Numerical Solutions of Partial Differential Equations II, Academic Press, New York, 1971, Ch. A new difference scheme for parabolic problems, pp. 327–350.

[2] K. B. Oldham, J. Spanier, The Fractional Calculus, Vol. 1047, Academic press New York, 1974.

[3] X. Chen, L. Wei, J. Sui, X. Zhang, L. Zheng, Solving fractional partial differential equations in fluid mechanics by generalized differential transform method, in: Multimedia Technology (ICMT), 2011 International Conference on, IEEE, 2011, pp. 2573–2576.

[4] A. A. Elbeleze, A. Kılıçman, B. M. Taib, Fractional variational iteration method and its application to fractional partial differential equation, Math. Probl. Eng. 2013 (2013) Article ID 543848 (10 pages).

[5] W. Schneider, W. Wyss, Fractional diffusion and wave equations, Journal of Mathematical Physics 30 (1) (1989) 134–144.

[6] M. Giona, H. E. Roman, Fractional diffusion equation for transport phenomena in random media, Physica A: Statistical Mechanics and its Applications 185 (1) (1992) 87–97.

[7] R. Metzler, J. Klafter, The random walk's guide to anomalous diffusion: a fractional dynamics approach, Physics reports 339 (1) (2000) 1–77.

[8] B. I. Henry, S. L. Wearne, Fractional reaction–diffusion, Physica A: Statistical Mechanics and its Applications 276 (3) (2000) 448–455.

[9] D. A. Benson, S. W. Wheatcraft, M. M. Meerschaert, Application of a fractional advection-dispersion equation, Water Resources Research 36 (6) (2000) 1403–1412.

[10] J. H. Cushman, T. R. Ginn, Fractional advection-dispersion equation: a classical mass balance with convolution-fickian flux, Water resources research 36 (12) (2000) 3763–3766.

[11] A. Atangana, E. Alabaraoye, Solving a system of fractional partial differential equations arising in the model of HIV infection of CD4+ cells and attractor one-dimensional keller-segel equations, Advances in Difference Equations 2013 (1) (2013) 1–14.

[12] P. Roul, Analytical approach for nonlinear partial differential equations of fractional order, Communications in Theoretical Physics 60 (3) (2013) 269.

[13] V. Méndez, D. Campos, F. Bartumeus, Anomalous diffusion and continuous-time random walks, in: Stochastic Foundations in Movement Ecology, Springer-Verlag, Berlin, 2014, pp. 113–148.

[14] I. Podlubny, Fractional differential equations, Mathematics in Science and Engineering, Academic Press, New York and London, 1998.

[15] A. M. Mathai, R. K. Saxena, The H-Function with Applications in Statistics and Other Disciplines, Wiley Eastern Ltd, New Delhi, 1978.

[16] S. B. Yuste, L. Acedo, An explicit finite difference method and a new von neumann-type stability analysis for fractional diffusion equations, SIAM J. Numer. Anal. 42 (5) (2005) 1862–1874.

[17] S. Shen, F. Liu, Error analysis of an explicit finite difference approximation for the space fractional diffusion equation with insulated ends, ANZIAM Journal 46 (2005) 871–887.

[18] F. Liu, P. Zhuang, V. Anh, I. Turner, K. Burrage, Stability and convergence of the difference methods for the space–time fractional advection–diffusion equation, Applied Mathematics and Computation 191 (1) (2007) 12–20.

[19] Y. Liu, L. Dong, R. Lewis, J.-H. He, Approximate solutions of multi-order fractional advection-dispersion equation with non-polynomial conditions, International Journal of Numerical Methods for Heat & Fluid Flow 25 (1).

[20] B. Jin, B. Li, Z. Zhou, Discrete maximal regularity of time-stepping schemes for fractional evolution equations, Numerische Mathematik 138 (1) (2018) 101–131.

[21] W. Deng, M. Chen, E. Barkai, Numerical algorithms for the forward and backward fractional feynman–kac equations, Journal of Scientific Computing 62 (3) (2015) 718–746.

[22] T. A. M. Langlands, B. I. Henry, The accuracy and stability of an implicit solution method for the fractional diffusion equation, Journal of Computational Physics 205 (2) (2005) 719–736.

[23] C. M. Chen, F. Liu, K. Burrage, Finite difference methods and a fourier analysis for the fractional reaction–subdiffusion equation, Applied Mathematics and Computation 198 (2) (2008) 754–769.

[24] D. A. Murio, Implicit finite difference approximation for time fractional diffusion equations, Computers & Mathematics with Applications 56 (4) (2008) 1138–1145.

[25] H.-l. Liao, Y.-n. Zhang, Y. Zhao, H.-s. Shi, Stability and convergence of modified du fort–frankel schemes for solving time-fractional subdiffusion equations, Journal of Scientific Computing 61 (3) (2014) 629–648.

[26] W. Yao, J. Sun, B. Wu, S. Shi, Numerical simulation of a class of fractional subdiffusion equations via the alternating direction implicit method, Numerical Methods for Partial Differential Equations 32 (2) (2016) 531–547.

[27] C. M. Chen, F. Liu, I. Turner, V. Anh, A fourier method for the fractional diffusion equation describing sub-diffusion, Journal of Computational Physics 227 (2) (2007) 886–897.

[28] G.-H. Gao, Z.-Z. Sun, H.-W. Zhang, A new fractional numerical differentiation formula to approximate the Caputo fractional derivative and its applications, Journal of Computational Physics 259 (2014) 33–50.

[29] Y.-N. Zhang, Z.-Z. Sun, H.-L. Liao, Finite difference methods for the time fractional diffusion equation on

non-uniform meshes, Journal of Computational Physics 265 (2014) 195–210.

[30] A. A. Alikhanov, A new difference scheme for the time fractional diffusion equation, Journal of Computational Physics 280 (2015) 424–438.

[31] P. Zhang, H. Pu, A second-order compact difference scheme for the fourth-order fractional sub-diffusion equation, Numerical Algorithms 76 (2) (2017) 573–598.

[32] R. H. Pletcher, J. C. Tannehill, D. Anderson, Computational fluid mechanics and heat transfer, CRC Press, 2012.

[33] F. S. Al-Shibani, A. I. Ismail, F. A. Abdullah, The Implicit Keller Box method for the one dimensional time fractional diffusion equation, Journal of Applied Mathematics & Bioinformatics 2 (3).

[34] S. A. Osman, Numerical solution methods for fractional partial differential equations, Ph.D. thesis, University of Southern Queensland (2017).

[35] F. Zeng, C. Li, A new crank–nicolson finite element method for the time-fractional subdiffusion equation, Applied Numerical Mathematics 121 (2017) 82–95.

[36] H. B. Keller, A new difference scheme for parabolic problems, in: B. Hubbard (Ed.), Numerical Solutions of Partial Differential Equations II, Academic Press, New York, 1971, pp. 327–350.

[37] P. Zhuang, F. Liu, V. Anh, I. Turner, New solution and analytical techniques of the implicit numerical method for the anomalous subdiffusion equation, SIAM Journal on Numerical Analysis 46 (2) (2008) 1079–1095.

[38] C.-M. Chen, F. Liu, V. Anh, I. Turner, Numerical schemes with high spatial accuracy for a variable-order anomalous subdiffusion equation, SIAM Journal on Scientific Computing 32 (4) (2010) 1740–1760.

[39] M. R. Spiegel, Laplace transforms, McGraw-Hill New York, 1965.

[40] M. R. Spiegel, Advanced mathematics, McGraw-Hill, Incorporated, 1991.

[41] C. N. Angstmann, I. C. Donnelly, B. I. Henry, Continuous time random walks with reactions forcing and trapping, Mathematical Modelling of Natural Phenomena 8 (2) (2013) 17–27.